Investigating the impact of coupling HARMONIE-WINS50 (cy43) meteorologie to LOTOS-EUROS (v2.2.002) on simulation of NO$_2$ concentrations over The Netherlands

Andrés Yarce Botero [1,2], Michiel van Weele [3], Arjo Segers [4], Pier Siebesma [2,3], and Henk Eskes [3]

[1]Faculty of Mathematical Physics, Delft University of Technology, Mekelweg 4, 2628 CD Delft EWI TuDelft, The Netherlands
[2]Faculty of Geoscience & Remote Sensing, Delft University of Technology, Stevinweg 1, 2628 CN, Delft, The Netherlands
[3]Royal Netherlands Meteorological Institute (KNMI), De Bilt, 3730 AE, The Netherlands
[4]Department of Air quality & Emissions Research, Netherlands Organisation for Applied Scientific Research (TNO), Princetonlaan 6, 3584 CB Utrecht, The Netherlands

Correspondence: Andrés Yarce Botero (a.yarcebotero@tudelft.nl)

Abstract. Meteorological fields calculated by Numerical Weather Prediction (NWP) Models drive offline Chemical Transport Models (CTM) to solve the transport, chemical reactions, and atmospheric interaction over the geographical domain of interest. HARMONIE (HIRLAM ALADIN Research on Mesoscale Operational NWP in Euromed) is a state-of-the-art non-hydrostatic NWP community model used at several European weather agencies to forecast weather at the local and/or regional scale. In this work, the HARMONIE WINS50 (cycle 43 cy43) reanalysis data set at a resolution of $0.025° \times 0.025°$ covering an area surrounding the North Sea for the years 2019-2021 was offline coupled to the LOTOS-EUROS (v2.2.002) CTM. The impact of using either meteorological fields from HARMONIE or from ECMWF on LOTOS-EUROS simulations of NO$_2$ has been evaluated against ground-level observations and TROPOMI tropospheric NO$_2$ vertical columns. Furthermore, the difference between crucial meteorological input parameters such as the boundary layer height and the vertical diffusion coefficient between the hydrostatic ECMWF and non-hydrostatic HARMONIE data has been studied, and the vertical profiles of temperature, humidity, and wind are evaluated against meteorological observations at Cabauw in The Netherlands. The results of these first evaluations of the LOTOS-EUROS model performance in both configurations are used to investigate current uncertainties in air quality forecasting in relation to driving meteorological parameters and to assess the potential for improvements in forecasting pollution episodes at high-resolutions based on the HARMONIE NWP model.

Keywords: WINS50, LOTOS-EUROS, HARMONIE (cy43), ECMWF, Offline coupling, TROPOMI

Copyright statement. TEXT

1 Introduction

Numerical Weather Prediction Models (NWP) provide the meteorological data required by Chemical Transport Models (CTMs) to resolve the emission, transportation, chemical reactions and other atmospheric interactions of pollutants throughout the spatio-temporal field of interest (Chang, 1980; El-Harbawi, 2013; Khan and Hassan, 2020). In this way, forecasts and (re-)analyses provided by NWP can be used for air quality forecasting, climate modeling, and environmental studies. The more precise the meteorological input data represents the atmospheric dynamics, the better the CTM represents pollutant transport, mixing, and the subsequent impact on surface air quality. Meteorological parameters related to transport and mixing have a direct impact on the surface air quality simulated by a CTM. A NWP model with a higher spatial resolution and better capabilities for resolving boundary layer turbulence dynamics and convective processes would provide a CTM with more accurate input parameters to predict the transport of pollutants, especially in the lowest kilometer(s) of the troposphere (Pielke and Uliasz, 1998).

However, it is important to note that the spatial resolution of the NWP model is not the only factor. Other factors may include the model's ability to accurately represent small-scale phenomena, turbulence dynamics, and convective processes (non-hydrostatic), compared to models that replace the vertical momentum equation by hydrostatic equilibrium (SAITO et al., 2007). Also, the quality of (operational) meteorological input is constantly improved through the data assimilation applied in NWP (Marseille and Stoffelen, 2017; Bengtsson et al., 2017; Lorenc and Jardak, 2018) which can reduce model uncertainty. Overall, it is important to carefully consider the uncertainty of the meteorological driving parameters in a CTM, as these parameters can significantly affect the accuracy and reliability of the air quality predictions.

HARMONIE (HIRLAM ALADIN Research on Mesoscale Operational NWP in Euromed) pertains to a script system and model configuration in meteorological modelling (Bengtsson et al., 2017; van Stratum et al., 2022). It is named for the scripting system utilized for data assimilation, observation handling, and operational processes in the Applications of Research to Operations at Mesoscale (AROME) model within the countries utilizing the High-Resolution Limited Area Model (HIRLAM). Additionally, "HARMONIE" denotes a particular setup of the AROME model. This updated configuration includes physical parameterizations specifically adapted for European conditions, particularly at northern latitudes. The operational high-resolution NWP model that is used in The Netherlands is generated with the HARMONIE model configuration (Haakenstad et al., 2021). The dataset that is used in this work is denoted as WINS50, which is a homogeneous HARMONIE reanalysis focusing on the North Sea region, developed by a consortium of Whiffle, TU Delft, and KNMI. The dataset covers the years 2019 to 2021 and has been created using HARMONIE cycle 43. It was evaluated for one year by (van Stratum et al., 2022), to show how and to what extent current wind farm structures in the north sea can cause effects on the meteorology at local to regional scales (Verzijlbergh, 2021; Kalverla et al., 2019; Baas et al., 2022).

LOTOS-EUROS (LOng Term Ozone Simulation-EURopean Operational Smog model) is a CTM that simulates the formation and transport of pollutants and trace gases in the atmosphere (Manders et al., 2017). The processes in the model include emission, advective transport, turbulent mixing, chemical reactions, wet- and dry deposition, and sedimentation. It is a CTM that is one of the members of the Copernicus Atmosphere Monitoring Service (CAMS) regional ensemble of CTMs that is used

to produce operational air quality forecasts over Europe and at a higher spatial resolution also over the Netherlands. In most applications, the model is driven by meteorological input from the European Centre for Medium-Range Weather Forecasts (ECMWF), but in this study, it has also been coupled with the HARMONIE NWP to provide a more comprehensive under-
standing of the formation and transport of air pollutants in the BeNeLux countries and North Sea region. In earlier studies, other meteorological drivers have been offline coupled to the LOTOS-EUROS model in one-way direction, including WRF (Escudero et al., 2019), and COSMO (Thürkow et al., 2021). A two-way coupling was implemented between the RACMO climate model and the CTM to provide information on the impact of meteorological conditions on air pollutants, and vice versa the impact of trace gases and aerosol on weather and climate via the radiation budget (Manders-Groot et al., 2011).

In a previous study (Ding, 2013), the impact of using HARMONIE (cy36) as meteorological driver for LOTOS-EUROS (v1.8) was compared with using the standard ECMWF meteorology as driver. That study found large differences in the meteorological variables obtained from the two drivers, especially at the coast, over forest regions, and in urban areas. However, the surface temperature, relative humidity, and wind patterns were found to be very similar between the models. Since this previous study, various updates and improvements have been made to both the HARMONIE NWP model and the LOTOS-EUROS CTM, which have involved into cycle 43 and version v2.2.002, respectively. Therefore, conducting a reassessment of their coupled performance is valuable.

Section 2 of this paper introduces the methodology used in the study. It includes a description of the two meteorological input fields in the configurations made for the coupling with the state-of-the-art version of LOTOS-EUROS used in this study. The coupling procedure between the meteorological driver and the CTM is explained in this section, along with the list of variables taken into account and any necessary calculations or assumptions for their correct ingestion into the CTM. Section 3 presents the results of the model simulations and their evaluation against ground-based observations and satellite-observed trace gas plumes. The comparison with observations is important to provide an independent assessment of the differences between the model simulations. The paper's final section, Section 4, discusses our results and provides the conclusions on the coupling of HARMONIE WINS50 NWP to LOTOS-EUROS to the extent these can be drawn from this study. Additionally, the potential improvement in high-resolution air quality forecasts that are offline driven by non-hydrostatic meteorological data is assessed.

2 Methodology: Coupling of Meteorological Drivers to the Chemical Transport Model

2.1 LOTOS-EUROS driven by ECMWF meteorology

LOTOS-EUROS is a large-scale three-dimensional CTM that simulates air pollution in the lower troposphere by solving a differential equation involving different operators, such as the transport operator, the chemical reaction operator, and the emissions/deposition operator. These operators are executed sequentially on a 3D set of grid cells covering the troposphere over the domain of interest. The horizontal advection is driven by horizontal winds (U, V) that are part of the meteorological input. When driven by ECMWF meteorology, the model calculates the vertical wind component (W) through the convergence and divergence of the horizontal winds. Turbulence driven vertical diffusion is modelled with a separate operator. The chemistry operator simulates the chemical production and loss terms from the different chemical reactions in the atmosphere. A Carbon

Bond Mechanism with 81 reactions (Schaap et al., 2008) is used to describe the gas-phase chemistry, and interaction with aerosols follows the ISORROPIA parameterisation (Fountoukis and Nenes, 2007). The dry deposition operator is parameterised following the resistance approach (Wichink Kruit et al., 2012). The wet deposition operator includes the below-cloud scavenging for gases (Schaap et al., 2004).

LOTOS-EUROS receives the ECMWF Integrated Forecasting System (IFS) meteorological fields on a regular longitude-latitude grid, which is then interpolated to the target grid that is either regular longitude-latitude too or uses a different projection. The vertical layers of the model are defined as a coarsening of the ECMWF hybrid sigma-pressure layers. The meteorological fields received from the ECMWF data include 3D fields of pressure, wind vectors, temperature, and humidity, as well as 2D fields of mixing layer height, precipitation rates, cloud cover, and other boundary layer and surface variables. A full overview of the meteorological fields is listed in Table 1 and described in the following section. A simulation with LOTOS-EUROS driven by ECMWF meteorology has been performed to serve as a reference for other simulations, and this will be referred to as "EC_LE".

2.2 LOTOS-EUROS driven by HARMONIE meteorology

The HARMONIE (HIRLAM ALADIN Research on Mesoscale Operational NWP in Euromed) is a non-hydrostatic convection-permitting Numerical Weather Prediction model (Engdahl et al., 2020; Clark et al., 2016). In a non-hydrostatic model, the vertical momentum equation is solved directly instead of applying the hydrostatic approximation, which frequently fails during extreme weather events (Gibbon and Holm, 2011). HARMONIE incorporates various dedicated sub-models to describe atmospheric processes. One of these models is SURFEX, which simulates processes such as temperature and water balance, radiation balance, and heat transport at the surface and in the soil (Viana Jiménez and Díez Muyo, 2019). The model accounts for various types of land surfaces and processes at and below the surface to describe the interaction between the atmosphere and the surface.

Similar to the ECMWF model, the HARMONIE model uses terrain-following hybrid sigma-pressure layers that are defined by surface pressure and hybrid level coefficients provided in the data files; Although the HARMONIE model could provide non-hydrostatic vertical advective fluxes, it was decided for this study to perform a coupling with HARMONIE based on the same approach as used for ECMWF variables (see also the discussion in Section 4).

The particular HARMONIE simulation for this study comes from the "WINS50" project. TUDelft, Whiffle, and KNMI have formulated the WINS50 project in the framework of the TKI Wind op Zee R&D 2019 (www.wins50.nl). The WINS50 model was run for 2019-2021 to produce winds undisturbed by wake effects (extension of the Dutch Offshore Wind Atlas DOWA) and disturbed winds (wake-DOWA). Kalverla et al. (2019) compared the simulations of the HARMONIE model over the North Sea with other models and with observations from a mast.

2.2.1 Coupling choices

To ensure successful coupling of the HARMONIE/LOTOS-EUROS system, a systematic approach was taken comparing the available ECMWF and HARMONIE fields. This involved classifying the variables into three categories: static, surface, and 3D

fields as shown in Table 1. The table was created to compare the variables' acronyms, units, and availability between the two systems. A simulation with LOTOS-EUROS driven by HARMONIE meteorology has been performed and this will be referred
120 to as "HA_LE". LOTOS-EUROS ingested the variables selected from HARMONIE that correspond to equivalent ECMWF variables based on the coupling choices specified in the next section. Second, decisions are taken about whether direct or indirect mapping should be done and what to do with missing variables. Third, the labeling and timestamp frequency and time bounds were corrected and the direct paths to find the data and meteorological files were generated for the LOTOS-EUROS files. Mapping half-level altitudes with half-level pressures with coefficients calculations was done using specific routines that
125 additionally flip the order of some of the required variables. Additionally, determining and converting variables needed in either accumulated or instantaneous format was another task. The coupling strategy for HARMONIE data in this study was defined with goal to emulate the coupling with ECMWF data, thus so far without using variables that are only available from HARMONIE. This thorough approach ensured that the (HA_LE) system is technically coupled, allowing for the generation of accurate and comprehensive CTM fields driven by this new source of meteorological information. Surface dewpoint and
130 friction velocity for grass were not available in the HARMONIE data. For the surface dewpoint the approximation in Lawrence (2005) was used. The friction velocity for grass was calculated by dividing the surface stress by air density and taking its square root.
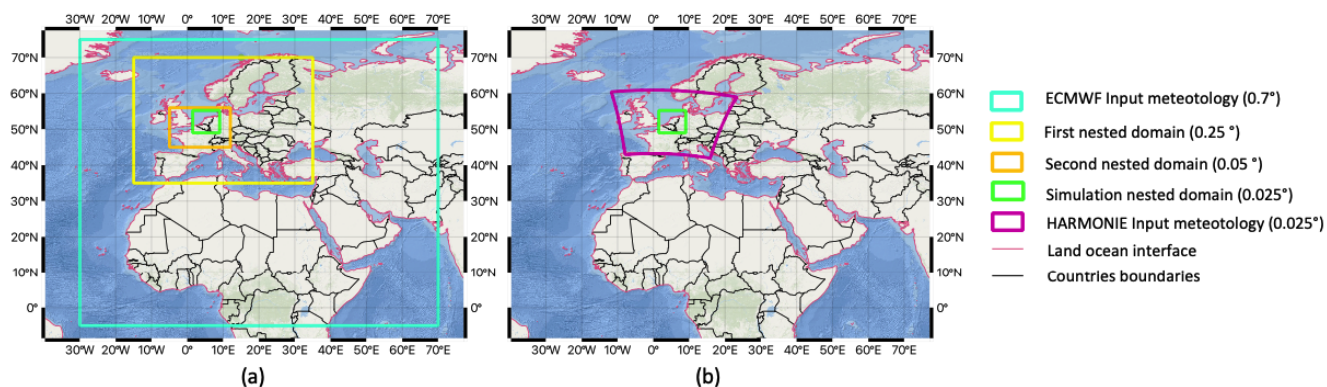
Figure 1. Simulation domains used for the LOTOS-EUROS simulations using ECMWF (left) or HARMONIE (right) meteorology. Both configurations use boundary conditions from CAMS. (map from Natural Earth collection (https://www.naturalearthdata.com/)

Table (2) and (3) shows the LOTOS-EUROS configuration settings for the simulations performed in this study. The simulations differ from each other in the meteorological driver. The rest of the parameters were not touched to attribute the
135 discrepancies only to the change in meteorology. The table lists the different parameters used in the two LOTOS-EUROS configurations, including the meteorological data source, the chemical boundary conditions, emissions, land use, horizontal resolution for the objective domain and for the nested domains, and the time step used for the simulations.

Table 1. Overview of the meteorological input data of the IFS (Integrated Forecasting System) provided by the ECMWF and the HARMONIE WINS50 meteorological variables used for the coupling to LOTOS-EUROS. The variables are divided into 1-Static surface fields, 2-Surface and other dynamic 2D variable, 3- three dimensional variables. HARMONIE variables with the symbol (*) were converted from instantaneous to accumulated.

ECMWF		HARMONIE		Units
Acronym	**Long name**	**Acronym**	**Long name**	
1- Static surface fields				
lsm	Land sea mask	lsm	Sea area fraction	[0,1]
orog	Orography	orog	Surface altitude	[m]
slt	Soil type	slt	Soil type	
2- Surface and other dynamic 2D model				
blh	Boundary layer height	zmla	Atmosphere boundary layer thickness	[m]
tsurf	Surface temperature	ts	Surface temperature	[K]
dsurf	Surface dewpoint		Calculated from hus and ts using Lawrence approximation	[K]
u10	10 meter wind vector	uas	Eastward Near-Surface Wind Velocity	[m s^{-1}]
v10	10 meter wind vector	vas	Northward Near-Surface Wind Velocity	[m s^{-1}]
sd	Snowdepth	snw	Surface snow amount	[m]
sstk	Sea surface temperature	sst	Sea surface temperature	[K]
swvl1	Volumetric soil water layer N	wsa_L01.P01	Volume Fraction Of Liquid Water In Soil Layer 1	[m^3 m^{-3}]
swvl2	Volumetric soil water layer N	wsa_L02.P02	Volume Fraction Of Liquid Water In Soil Layer 2	[m^3 m^{-3}]
swvl3	Volumetric soil water layer N	wsa_L03.P03	Volume Fraction Of Liquid Water In Soil Layer 3	[m^3 m^{-3}]
swvl4	Volumetric soil water layer N	wsa_L04.P04	Volume Fraction Of Liquid Water In Soil Layer 4	[m^3 m^{-3}]
tcc	Total cloud coverage	clt	Total cloud fraction	[0 1]
zust	Friction velocity grass		Calculated from wind with square(Tauu+Tauv)/density	
sshf	Surface sensible heat flux	hfss	Accumulated Surface Upward Sensible Heat Flux	[J m^{-2}]
slhf	Surface latent heat flux	hfls_eva	Accumulated Upward latent flux of evaporation (*)	[J m^{-2}]
cp	Convective precipitation	prrain	Accumulated rain (*)	[kg m^{-2}]
lsp	Large scale precipitation	prrain	Accumulated rain (*)	[kg m^{-2}]
sf	Snowfall	prsn	Snowfall amount (*)	[kg m^{-2}]
ssrd	Surface solar radiation downwards	rsds	Accumulated Surface Downwelling Shortwave Radiation (*)	[J m^{-2}]
sp	Surface pressure	ps	Surface air pressure	[Pa]
3- Dynamic model 3D fields				
hp	pressure at layer interfaces	hp	pressure at layer interfaces	[Pa]
t	Temperature	ta	Air temperature	[K]
q	Specific humidity	hus	Specific humidity	[kg kg^{-1}]
v	v component of wind	va	Northward wind velocity	[m s^{-1}]
u	u component of wind	ua	Eastward wind velocity	[m s^{-1}]
cc	Cloud cover	clt	Total Cloud Fraction	[0-1] [kg kg^{-1}]
clwc	Specific cloud liquid water content	clw	Cloud water	[kg kg^{-1}]

Table 2. LOTOS-EUROS configuration settings for the simulations in this work with HARMONIE meteorology input. Coordinates of the domain presented in [Lat N, Lon E].

Characteristic	HARMONIE Details
Simulation Periods	1 April to 30 April 2019
Meteorology	HARMONIE WINS50; temp.res: 1h; spat.res: 0.025°
Initial and Boundary Conditions	CAMS (D1); temp.res: 1h; Spat.Res: 0.9°
Anthropogenic Emissions	CAMS; spat.res: 0.1°
Biogenic Emissions	MEGAN; spat.res: 0.1°
Fire Emissions	CAMS GFAS; spat.res: 0.1°
Land Use	CLC 2012; spat.res: 0.01°
Topography	GMTED2010. Spat.res: 0.002°
HARMONIE WINS50 (Lagrangian projection)	[-8.5°, 43°] x [16°, 42°]x[23°, 59°] x [-12°, 61°]
Objective simulation grid [Lat] x [Lon] (Both configurations)	[49°, 13.27°] x [1.5°, -65.94°]

Table 3. LOTOS-EUROS configuration settings for the simulations in this work with the ECMWF meteorology input. Coordinates of the domain presented in [Lat N, Lon E].

Characteristic	ECMWF Details
Simulation Periods	1 April to 30 April 2019
Meteorology	ECMWF; temp.res: 1h; spat.res: 0.7°
Initial and Boundary Conditions	CAMS (D1); temp.res: 1h; Spat.Res: 0.9°
Anthropogenic Emissions	CAMS; spat.res: 0.1°
Biogenic Emissions	MEGAN; spat.res: 0.1°
Fire Emissions	CAMS GFAS; spat.res: 0.1°
Land Use	CLC 2012; spat.res: 0.01°
Topography	GMTED2010. Spat.res: 0.002°
ECMWF [Lat N x Lon E]	[-5°, 75°] x [-30°, 70°]
First ECMWF Nested Domain [Lat] x [Lon]	[35°, 70°] x [-15°, -35°]
Second ECMWF Nested Domain [Lat] x [Lon]	[45°, 18°] x [5°, -60°]
Objective simulation grid [Lat] x [Lon] (Both configurations)	[49°, 13.27°] x [1.5°, -65.94°]

2.2.2 Computational aspects

The Figure (1) shows the spatial configurations of the LOTOS-EUROS CTM used with a specific meteorology drivers. The configuration for using ECMWF meteorology on panel (a) has three nested domains, which is common practice for more precise modelling of atmospheric conditions in areas with coarse meteorological information. The configuration for the HARMONIE meteorology on the panel (b) only uses one domain; in this case there is no nesting needed because the input resolution of the
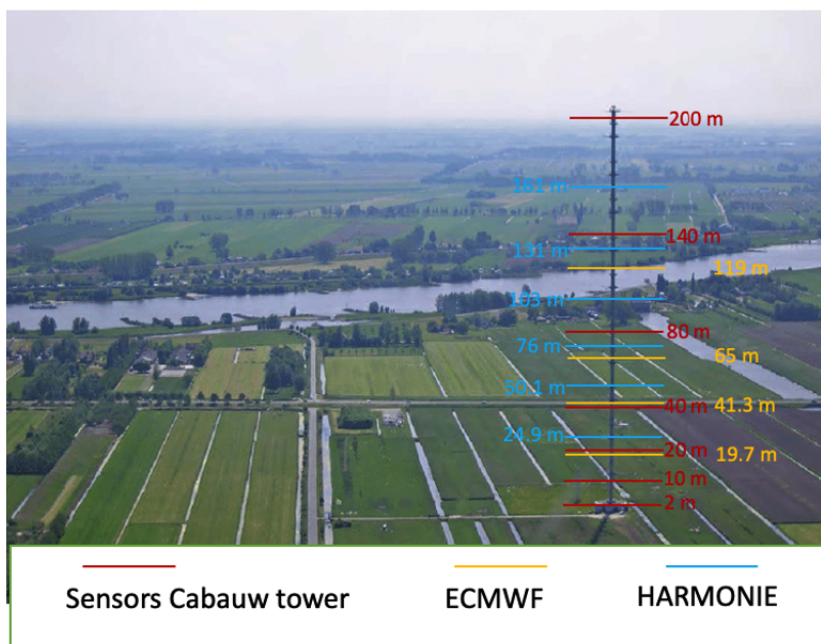
Figure 2. Image of the Cabauw tower (lat 51.96° N, lon 4.89°W) with in red the locations of the meteorological sensors, and in yellow and blue the interfaces between the ECMWF and HARMONIE model layers. Aerial photo image modified from (Apituley et al., 2008).

meteorology already has the intended resolution for the CTM; the green box is the actual domain for the "final" simulations which is the same for both configurations.

145   The objective of the simulations is to obtain CTM simulations at 0.025°over The Netherlands and the North Sea. For this, the HARMONIE/LOTOS-EUROS coupling uses only one nested simulation, while the ECMWF/LOTOS-EUROS coupling uses three nested simulations. The single nested configuration provides significant computational benefits. The computational resources required for the single-level approach are a factor four lower than the costs of the three-level nesting approach, while maintaining comparable accuracy in the results. This was achieved because the resolution of HARMONIE input meteorology

150   were comparable in terms of spatial resolution of the simulation domain objective, and could be used directly at the target grid. The reduction in the number of nested domains led to a substantial reduction in the computational resources required for the simulation, enabling us to tackle larger and more complex problems with the same resources. Overall, the results of our study highlight the significant benefits of using a nested domain simulation with fewer levels of nesting and demonstrate its potential as a powerful tool for numerical simulations.

155   **2.3   Observations**

During April 2019, we observed two distinct weather patterns which changed the atmospheric conditions within the month and could be attributed to variations in wind speed and direction. Evidence for the change in meteorological conditions is provided

by the directionality of plumes captured by satellite instruments, as illustrated in the subsequent figures 1 and 2 in the appendix section. We compared the model simulations with ground-based observations derived from the air quality network during these periods in April 2019.

2.3.1 Cabauw meteorology observations

Meteorological observations from the Cabauw site have been used to validate the meteorological data sets used in this study. The 213-meter tall KNMI-mast in Cabauw (Figure 2) generates continuous and stable meteorological observations at a location with homogeneous characteristics in a central part of The Netherlands. This site is located in a flat terrain with an elevation of 0 meters above sea level and has been used to validate models, satellite instruments, and other meteorological sensors (Bosveld et al., 2020). The surrounding area is mainly used for agriculture purposes; although the Cabauw tower is located in a rural area, small towns and villages are nearby. For this study observations were downloaded from KNMI for the period April-August 2019. The data comes in 10-minute sampling intervals and contains air temperature, dew point temperature, specific humidity, wind speed, and wind direction.

2.3.2 Surface concentration pollutants information

Surface observations NO_2 have been used to validate the LOTOS-EUROS simulations. The NO_2 data was downloaded for the ground stations at different places in the Netherlands from www.luchtmeetnet.nl. Different locations in the country were chosen to compare the two NO_2 LOTOS-EUROS systems with the different meteorological data sets in a representative way. This data is provided by *Rijksinstituut voor Volksgezondheid en Milieu* (RIVM). The RIVM is accredited for air quality measurements of SO_2, NO, NO_2, O_3, $PM_{2.5}$ and PM_{10} by the Dutch "Raad voor Accreditatie (RvA)" according to NEN-EN-ISO/IEC 17025:2018.

2.3.3 TROPOMI

The TROPOspheric Monitoring Instrument (TROPOMI) is the satellite instrument on board the Copernicus Sentinel-5 Precursor (S5p) satellite. S5P is a low-Earth polar orbit satellite. The polar orbit and wide coverage of the scanner provide almost daily global coverage, with a spatial pixel resolution of 5.5 x 3.5 km^2. The TROPOMI instrument is a spectrometer sensing ultraviolet (UV), visible (VIS), near (NIR), and short-wavelength infrared (SWIR) wavelengths to monitor Ozone (O_3), Methane (CH_4), Formaldehyde (CH_2), Aerosol, Carbon Monoxide (CO), Nitrogen Dioxide (NO_2), and Sulfur Dioxide (SO_2). The NO_2 retrievals used in this study are retrieved from a wavelength range of 405–465 nm (spectral band 4). The Royal Netherlands Meteorological Institute (KNMI) created the TROPOMI NO_2 retrieval method based on the DOMINO NO_2 retrieval algorithm employed on the Ozone Monitoring Instrument (OMI) precursor instrument (Boersma et al., 2011). In this work, the NO_2 retrievals from TROPOMI were used to select a simulation period with well-defined characteristics of the tropospheric NO_2 concentrations and to see if the different model simulations are able to represent this.
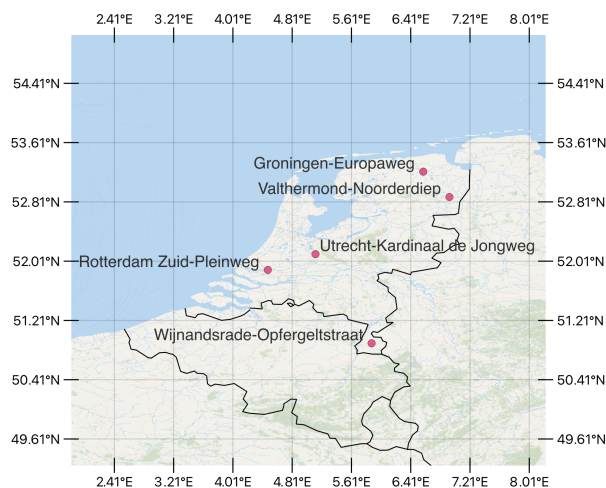
Figure 3. Map of the Netherlands with the air quality locations of the selected points to compare the simulations. Base map from Natural Earth collection (https://www.naturalearthdata.com/)

3   Results

3.1   Meteorology fields evaluation

190   Figure 2 provides an illustration of the Cabauw tower, with the positions of the sensors and the interfaces between ECMWF and HARMONIE model layers to illustrate the height of the varying model levels for comparison. This information is essential for validating the models' height levels and identifying potential sources of discrepancies between the model outputs and the observations in the vertical domain.

A comparison between the observed and simulated temperatures at different levels is shown in Figure 4. Panel (a)displays
195   the time series of temperature from the ECMWF meteorology compared withobservations at Cabauw at different levels. The comparison shows that there are some differences between the two datasets at certain levels, particularly during nighttime. The daily cycle is in phase, but there are minor differences in magnitude.

Figure (4) shows the daily cycle for three levels of the two meteorology input data sets as provided to LOTOS-EUROS compared to observations at the Cabauw tower. The values show minor differences, which gives technical trust in the model
200   configurations. For the height of 140 m from the Cabauw tower, the HARMONIE meteorology shows a bit lower RMSE, showing a bit better agreement with the observations.

Figure (5) shows a comparison of the wind speed and wind direction at the resolution of LOTOS-EUROS for the two meteorological input data sets. For the chosen time, the fields are very similar, although there are some differences in the details. Although small, such differences may contribute to differences in air quality at specific locations and variations in wind
205   (direction) could be important when comparing model simulations with air quality observations from measurement sites. An
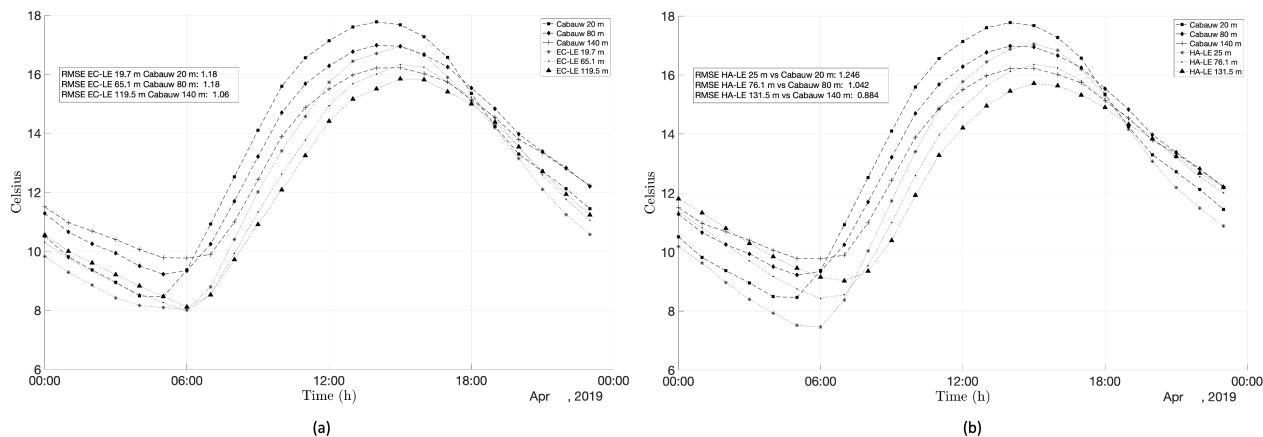
Figure 4. The daily temperature cycle from ECMWF (a) and HARMONIE (b) meteorological data and the Cabauw observations at different LOTOS-EUROS simulation levels. The RMSE for different levels is shown for the two input meteorological data sets in comparison to the temperature from the sensors in the tower

extensive validation of the meteorological variables of the HARMONIE model against Cabauw vertical profile observations can be found in (Knoop et al., 2020).

3.2 Comparison of concentration fields

Figure (6) compares the simulated surface concentrations of NO_2 for the EC_LE (a and d) and HA_LE (c and f) model
210   configurations at two different moments: April 3, a day without a dominant wind direction (upper panels), and April 12, a day with a clear westward directed wind field. To gain further insight into the differences between the two configurations, the fractional difference ((EC_LE)-(HA_LE))/(EC_LE) is shown in panels (b and e). These fractional differences clearly show that the (HA_LE) model configuration produces similar but different NO_2 concentrations compared to the (EC_LE) configuration at the chosen time. This reveals a difference in wind direction in the meteorological drivers which could impact
215   the simulated time series at any location. This suggests that wind direction can play a crucial role in the transport and diffusion of NO_2 in the atmosphere and could affect the simulated concentrations.

The experiment demonstrates that air mass characterization, e.g. informed by NO_2 concentration plume structures, may reveal significant discrepancies between HA_LE and EC_LE simulations. Evidence is provided by the statistical metrics, quantifying areas of over and underestimation. Clearly, small-scale wind direction changes have an impact on NO_2 pollutant
220   transport, and contribute to variations in pollutant concentrations across different regions. Accurate meteorological inputs are invaluable for LOTOS-EUROS simulations, particularly for the understanding of time series of NO_2 a the stations of the gound network in the Netherlands.

An example of the tropospheric column of NO_2 for the (EC_LE) and (HA_LE) configurations, as well as the tropospheric column retrieved from the TROPOMI satellite instrument is shown in Figure (7) for a single snapshot for 22 April 2019. Panel
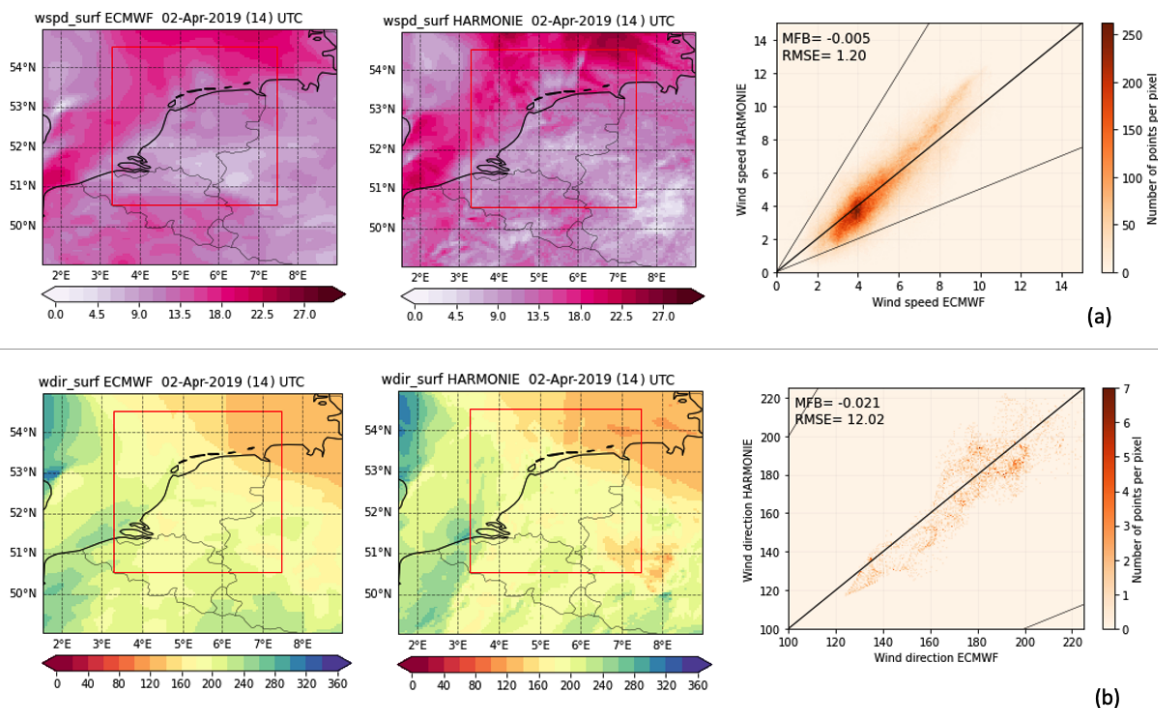
Figure 5. Instantaneous of surface wind speed [m/s] (wspd_surf) and direction [°] (wdir_surf) from ECMWF or HARMONIE meteorological fields interpolated to the LOTOS-EUROS grid. The scatter density plots on the right compare the values enclosed by the red square. Base maps from (http://www.gadm.org/)

225 (a) of the figure shows the tropospheric column of NO_2 for the (EC_LE) configuration, while panel (b) shows the tropospheric column of NO_2 for the (HA_LE) configuration. Panel (c) shows the tropospheric column of NO_2 obtained from the TROPOMI satellite retrieval.

The comparison reveals that the (HA_LE) configuration produces a tropospheric column of NO_2 that is slightly more similar to the TROPOMI satellite retrieval, particularly in regions with high NO_2 concentrations. The difference with the

230 EC_LE simulation is due to a slight difference in wind direction in the HARMONIE configuration, which affects the transport and diffusion of NO_2 emissions in the atmosphere. In addition to revealing differences in NO_2 concentrations between the two model configurations and the satellite retrieval, the images in Figure (7) show different details over the maps. Specifically, the maps illustrate the locations of coal and gas power stations, oil rigs and pipelines, principal airports, and roads across the Netherlands. These details are important to consider in atmospheric chemistry modeling, as they can help to identify potential

235 sources of NO_2 emissions and inform policy decisions related to air quality management.

Figure 8 shows a comparison between the NO_2 simulations and observations at three stations within the national air quality network. The locations compared are marked in Figure 7 with a red star: Station Utrecht Kardinaal de Jongweg (a) is located
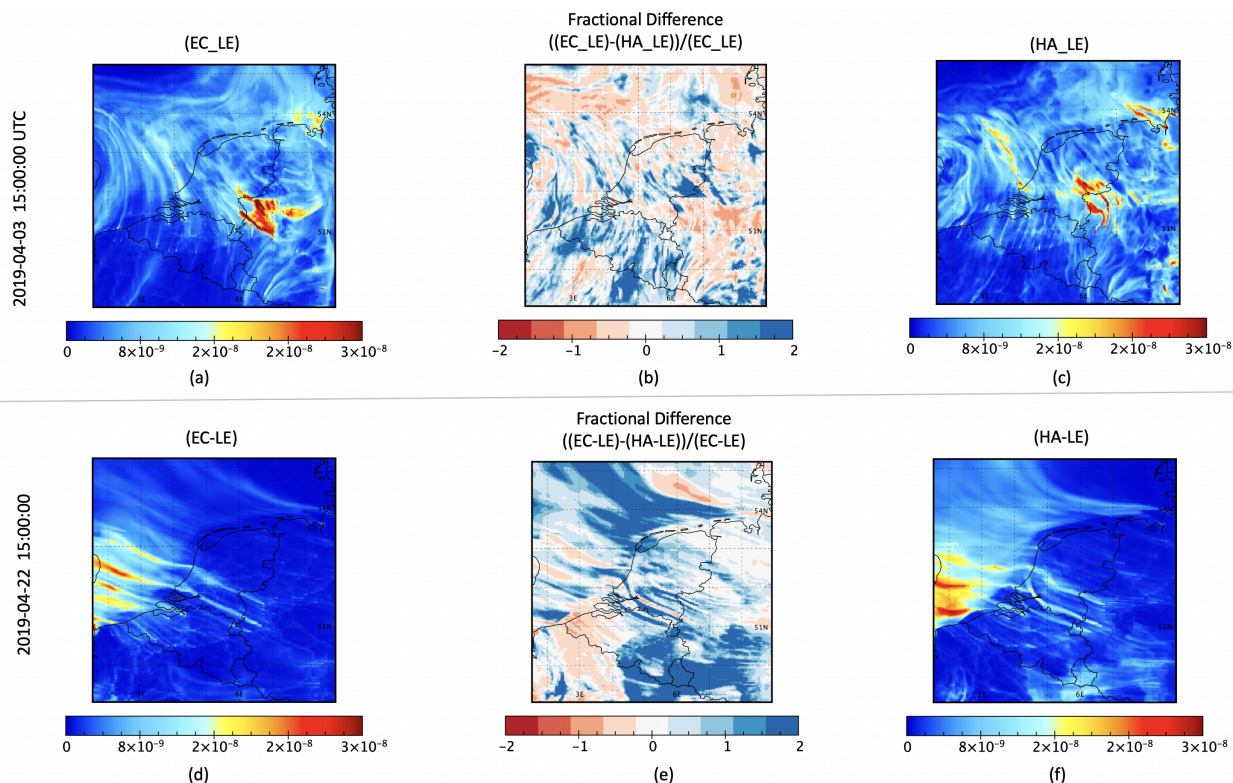
Figure 6. Maps of volume mixing ratio of surface NO$_2$ [mol mol^{-1}] at 2019-04-03 (top) and 2019-04-12 (bottom) at 15:00 UTC, from either EC_LE (a and d) or HA_LE (c and f) configurations. The middle panels (b and e) shows the fractional difference. Base maps from (http://www.gadm.org/)

in a central part of the country; Rotterdam Zuid-Pleinweg (b) is located in the city of Rotterdam and is characterized by high levels of pollutants, also due to the nearby presence of the harbor and refineries activities, and Valthermond Noorderlep (c) is located in a more rural area. The standard deviation between the grid cell where each station is located and its neighbouring cells is added to the simulation time series to have a notion of the representative error of these site comparisons. Three statistics (RMSE, MFB, Correlation) are presented for each configuration in each location. The highest correlations with the observations over the full time period are obtained using the HARMONIE high-resolution meteorology. The lower panel of this figure shows the vertical diffusion coefficient K$_z$ between the surface and the second LOTOS-EUROS model layer which offers additional insights into the analysis of surface air quality observations. Kz values are high over the Rotterdam Zuid-Pleinweg station; for the other two stations, Utrecht Kardinaal de Jongweg and Valthermond Noorderlep, lower Kz values are found but with relatively higher values in the HARMONIE model configuration which suggest a locally higher vertical mixing in this model configuration.

Table 4. Names and labels are displayed in Figure 7 for the largest emitters in the Netherlands, categorized by factories, refineries, and power plants using coal and gas as sources.

Factories and Refineries					
Tata Steel	1	Terneuzen	5	Gunvor Petroleum	9
Chemelot	2	Yara Sluiskil	6	Vitol/Koch/VPR Energy	10
DOW Benelux	3	Exxon Mobile Rotterdam	7		
Shell Rotterdam	4	BP	8		
Power plant (coal)					
Maaslavkte	11	Hemweg 8	13	Eemshaven	15
Maaslavkte MPP3	12	Gelderlan	14		
Power plant (gas)					
Sloe	16	Ijmond	20	HARCULO	24
Rijnmond II	17	Centrale Merwedekanaal	21	Magnum	25
ELSTA	18	Maxima	22	Eems	26
Diemen 33	19	Flevo	23	Delesto	27

The transversal cut over the Netherlands in Figure (9) shows a comparison between the (EC_LE) configuration in the upper panel and the (HA_LE) NO_2 fields in the panel below. The figure indicates notable differences in the NO_2 concentration fields produced by the two model configurations in both the NO_2 columns and the value of the K_z diffusion coefficient at the layer interfaces. The planetary boundary layer height is shown in all pictures with a shaded blue line. Here, the HARMONIE provides a more complex structure that impacts the modelled vertical mixing. In panel (a), the (EC_LE) configuration shows lower NO_2 concentrations compared to panel (b), where the (HA_LE) configuration produces higher NO_2 concentrations. Note that the differences with the observations may be attributed to the (different) meteorological drivers as well as to the (identical, but uncertain) emission data in the two model configurations. Both meteorology and emission and chemistry uncertainties can affect the ability of a CTM to simulate observations of atmospheric polutants.

Overall, our comparison of the two model configurations highlights the importance of an appropriate model configuration when evaluating NO_2 concentrations in a given region with a CTM at a given spatial resolution. More research is needed to investigate the specific factors that contribute to the differences between the two model configurations for LOTOS-EUROS and to determine which configuration is more accurate for simulating NO_2 concentration in the Netherlands. Figure 10 compares both configurations for a mean of April for 4 levels of the NO_2 concentration and the diffusion coefficient.

The HARMONIE atmospheric model stands out with its enhanced structure and distinct field shape compared to the ECMWF. However, it exhibits a discrepancy when simulating the boundary layer height, overestimating it compared to real-world observations. This disparity significantly affects air pollutant concentrations, particularly at higher lvels in the atmosphere. The higher simulated boundary layer height in HARMONIE allows pollutants to be transported to higher altitudes, leading tochanges in chemical reactions and the formation of secondary pollutants. The amount of upward mixing affects
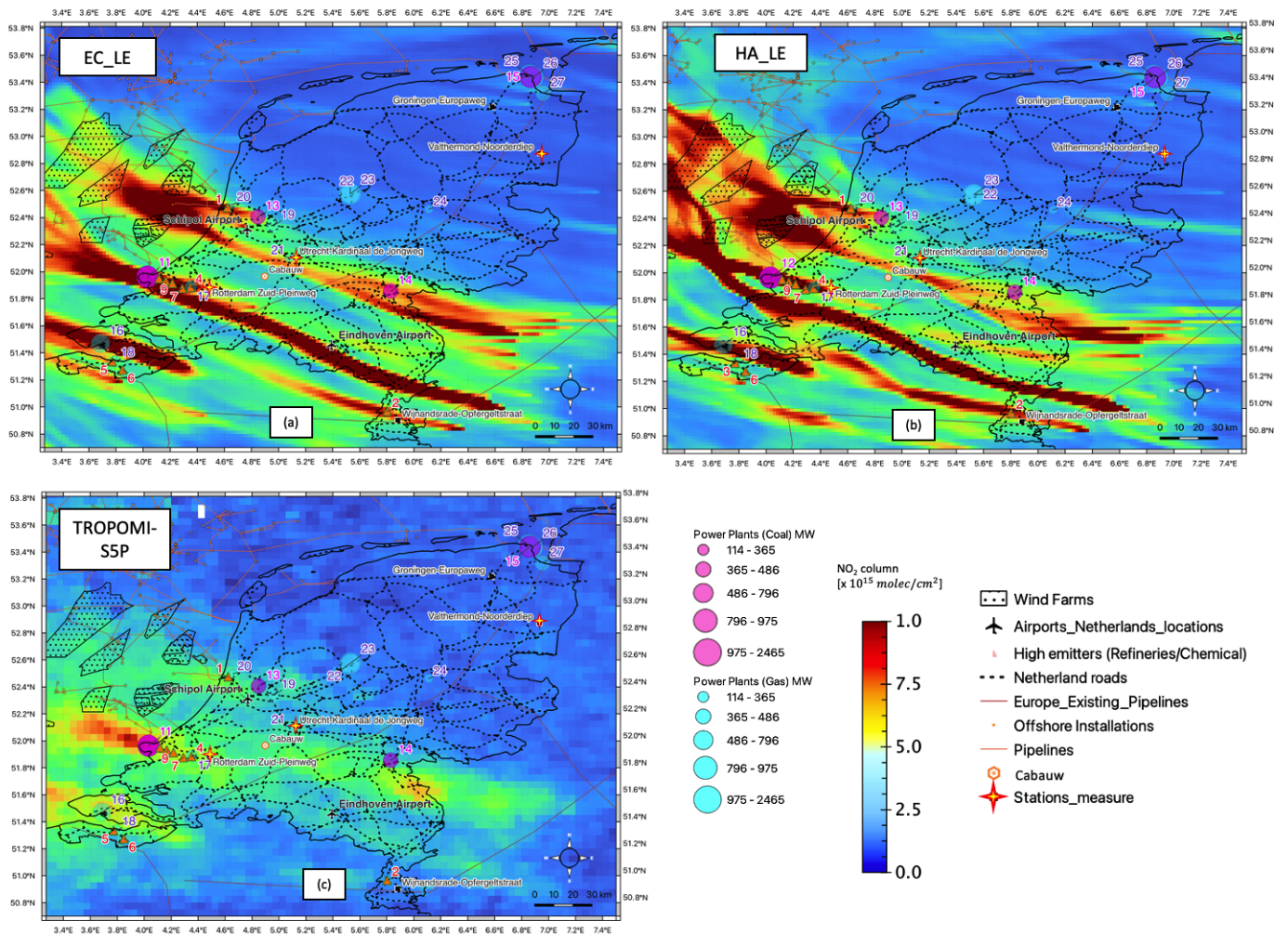
Figure 7. Comparison between the tropospheric columns of NO$_2$ (EC_LE) (a) and (HA_LE) (b) for the overpass time at 14:00 local of TROPOMI of which the retrieved tropospheric columns are shown in (c) for 22 April 2019. Large sources of NO$_x$ such as power plants, principal airports, and main roads are marked. The ground observation stations depicted with a star are the stations shown in Figure 8. Base maps from (http://www.gadm.org/) and information from (https://emodnet.ec.europa.eu/en/human-activities).

regional air quality, climate, and the understanding of long-range pollutant transport. Accurately representing the boundary layer height is therefore crucial for reliable air quality forecasts and the assessment of (surface) pollutant impacts. Resolving this issue requires further research and refinement of the model's parameterizations and processes related to boundary layer dynamics, enabling improved simulations of pollutant vertical dispersion into different atmospheric layers.

The comparison between the LOTOS-EUROS simulated retrieval of the tropospheric column of NO$_2$ and the TROPOMI average tropospheric vertical column which corresponds to the input needed for the data assimilation stage are shown in Figure
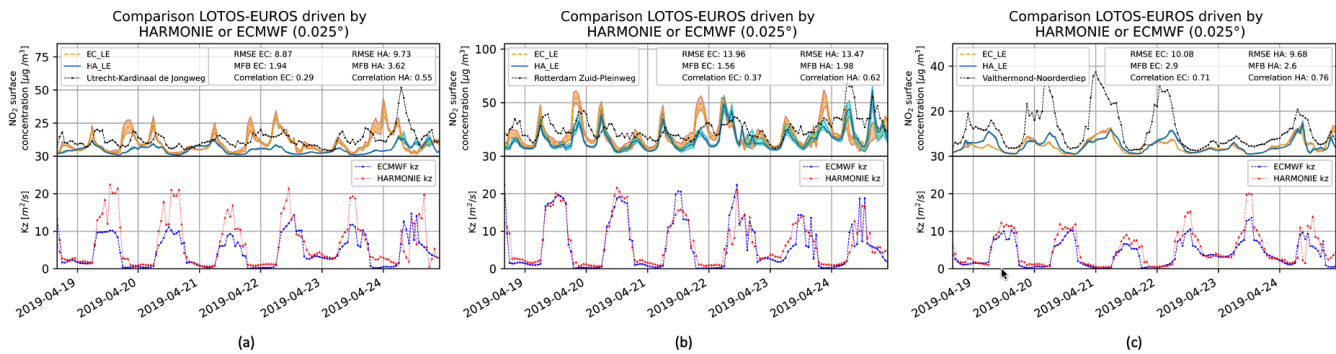
Figure 8. Comparison between NO$_2$ observations and simulations at 3 air quality stations from the national network: (a) Utrecht Kardinaal de Jongweg, (b) Rotterdam Zuid=-Pleinweg, and (c) Valthermond Noorderlep. Shaded area represents the standard deviation between the grid cell where the station is located and the surrounding cells. The below panel shows the simulations of the vertical diffusion coefficient K$_z$ between the surface and second LOTOS-EUROS model layer.
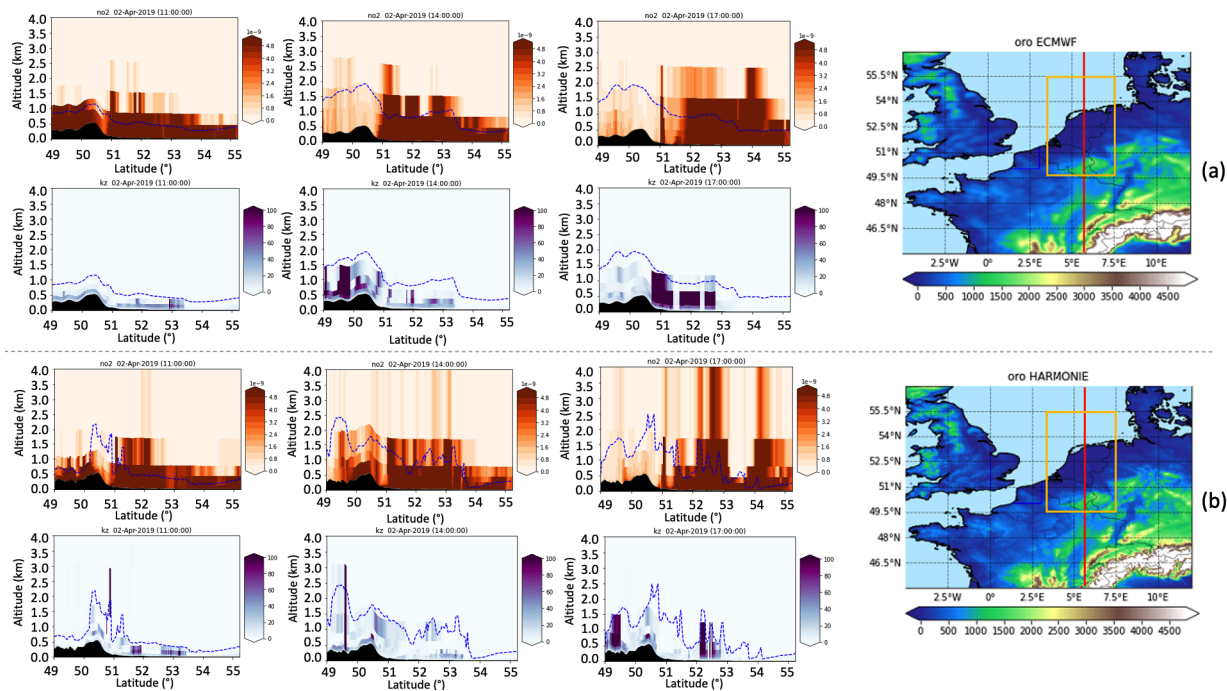
Figure 9. (a) Transversal cuts on longitude (6.2 $^\circ$ E) over the Netherlands comparison between the (EC_LE) configuration and (b) the (HA_LE) NO$_2$ concentration fields. The dashed blue lines correspond to the planetary boundary layer in the models. The panels on the right show each of the transversal cuts. Base maps from (http://www.gadm.org/).
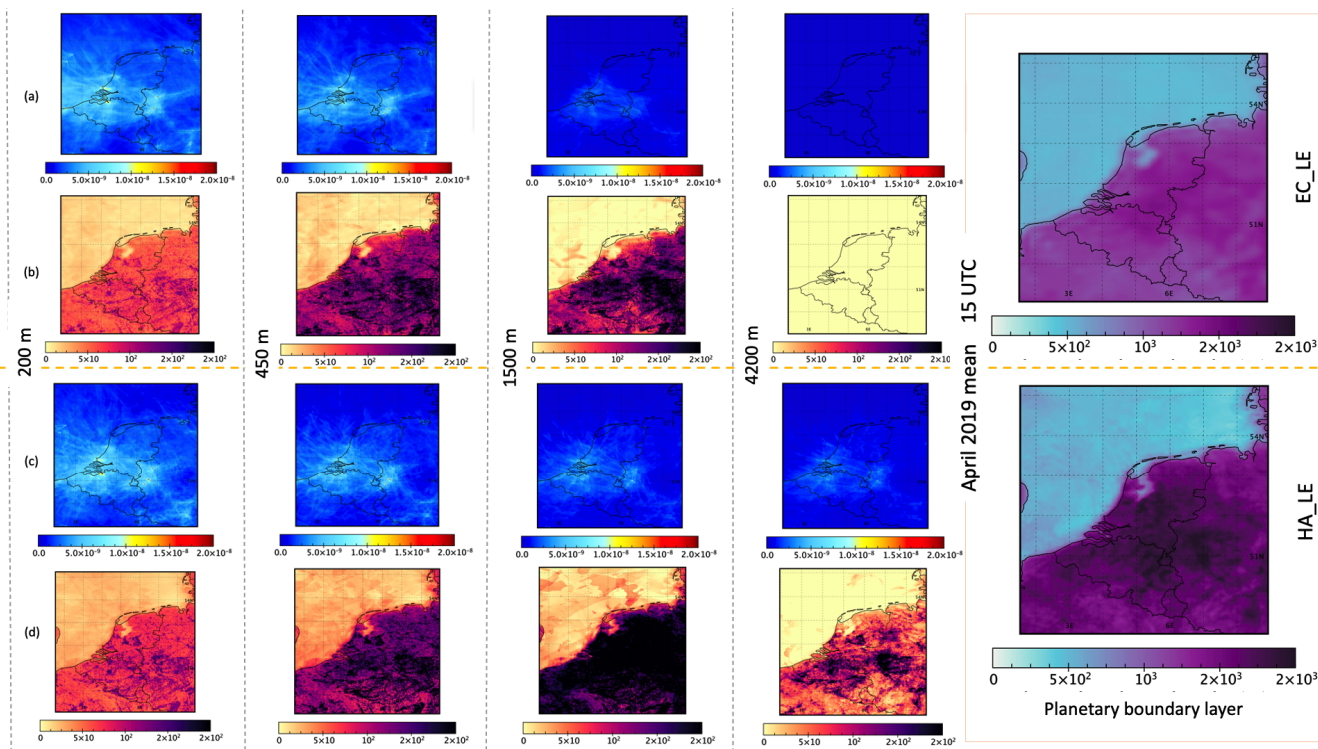
Figure 10. April mean (15 UTC) NO$_2$ concentration fields [mol mol^{-1}] and Kz [m^2 s^{-1}] at 200, 450, 1500, and 4200 m altitude (a,c) for EC_LE and (b,d) for HA_LE. Base maps from (http://www.gadm.org/).

(11). Panel (a) of 11shows the TROPOMI average tropospheric vertical column Yr product, panel (c) the LOTOS-EUROS simulated retrieval of the tropospheric column of NO$_2$ Ys, while panel in the middle show the difference.

4 Discussion

In this study two meteorological models which have different features served as input for the LOTOS-EUROS chemical transport model. The hydrostatic nature of a meteorological model as ECMWF refers to the assumption that the atmosphere is in a state of hydrostatic equilibrium, meaning that the vertical pressure gradient balances the gravitational force. In this configuration, the atmospheric equations used by the model do not include the effects of non-hydrostatic processes, such as wind, turbulence, and gravity waves. In contrast, a non-hydrostatic meteorological model allows for including non-hydrostatic processes in the atmospheric equations. This can provide a more accurate representation of the mixing dynamics of the atmosphere, especially in regions where these processes are significant, such as near the coast, over forests, and in urban areas.

The choice of a hydrostatic or non-hydrostatic meteorological configuration can significantly impact the performance of a chemical transport model. A hydrostatic configuration may be sufficient in some cases, but a non-hydrostatic configuration may be necessary to better represent the transport of pollutants in the atmosphere accurately. Overall, it is essential to carefully
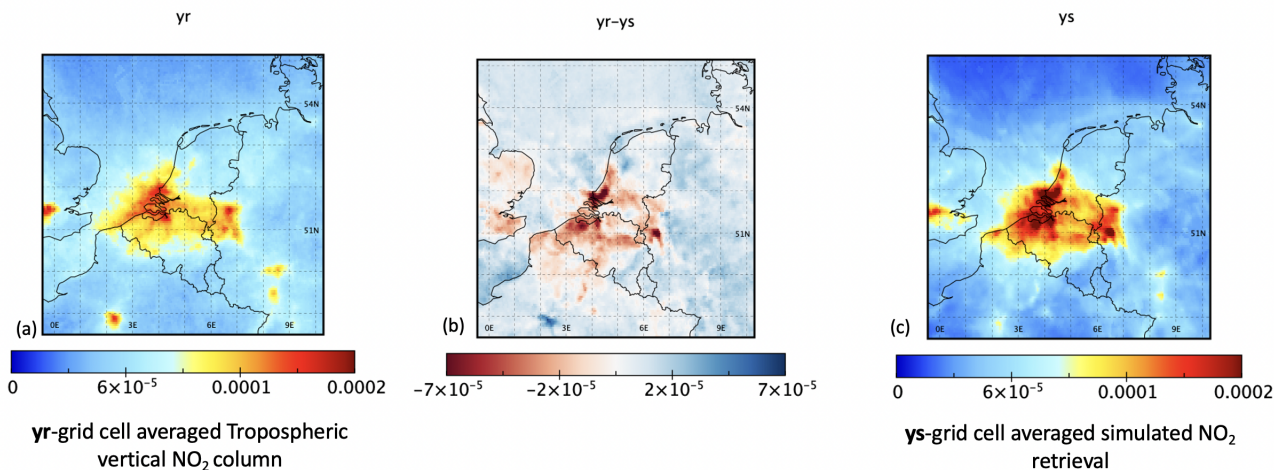
Figure 11. Comparison between the LOTOS-EUROS simulated retrieval of the tropospheric column of NO$_2$ Ys and the TROPOMI average tropospheric column Yr. Base maps from (http://www.gadm.org/)

consider the meteorological model's capabilities and the study region's specific characteristics when choosing a hydrostatic or non-hydrostatic configuration for a chemical transport model. This can ensure that the model can accurately represent the transport of pollutants and quantify air quality.

290   In this study, the vertical velocity fields in LOTOS-EUROS are calculated using the convergence and divergence of the horizontal winds from the meteorological model. This allows the model to simulate the effects of vertical motion in the atmosphere on the transport of pollutants.Uncertainties in the vertical transport and mixing cause that a CTM may not accurately represent the vertical motion of pollutants in the atmosphere. This can lead to significant errors in the model's predictions of the distribution and impact of pollutants on air quality. Other models, such as CHIMERE, recently evaluated a new vertical advection

295   mechanism to improve the vertical transport and a new vertical advection scheme that strongly reduces excess vertical diffusion (Menut et al., 2021).

Using high-spatial resolution meteorology in a CTM like LOTOS EUROS can improve the accuracy and reliability of the model simulations. High-resolution meteorological data provides more detailed information about the atmosphere's wind, temperature, pressure, and humidity conditions, which can be used to simulate the movement of pollutants and trace gases more

300   accurately. In particular, high-resolution meteorology can provide more accurate representations of the effects of small-scale atmospheric processes, such as turbulence and convection. This can improve the model's ability to simulate the distribution and impact of pollutants on air quality and can provide more detailed and helpful information for air quality forecasting.

The input meteorological information is part of the CTM model error, and should be included in the uncertainty description when assimilating observations. The following step is the preparation for the assimilation experiments using satellite column

305   measurements. Figure (11) shows the two products needed to perform the assimilation, the difference between both provide the input to correct in any of the data assimilation techniques. It is important to carefully consider the model configuration and

meteorological factors such as vertical mixing in a CTM for the potential benefits of satellite remote sensing data in improving the accuracy of the modelled NO_2 concentrations. There might be significant differences between the simulated and observed products, in particular in regions with high NO_2 concentrations. Underlying model uncertainties due to e.g. vertical mixing are important to consider in the data assimilation stage, as they can impact the accuracy of the assimilated data and, ultimately, the accuracy of the analysis modelled NO_2 concentrations.

5 Conclusions

This study explores the coupling of meteorological data from the HARMONIE (cy43) model with the LOTOS-EUROS Chemical Transport Model (CTM) to simulate NO_2 concentrations, comparing these results with simulations that utilize ECMWF meteorological data. The research seeks to evaluate the performance and accuracy of these different meteorological couplings in predicting NO_2 levels. A general comparison between the two setups reveals that both meteorological variables and NO_2 simulations are comparable, indicating a level of technical consistency between the HARMONIE and ECMWF configurations.

Despite the overall comparability, notable differences emerge in the vertical column concentrations of NO_2. Specifically, the HARMONIE configuration exhibits higher values in the upper layer of the atmosphere compared to the ECMWF setup. This difference is at least partly attributed to the vertical diffusion coefficients and planetary boundary layer height, highlighting the sensitivity of NO_2 dispersion to model-specific meteorological parameters. Our analysis reveals that HARMONIE provides a more detailed structure for meteorological drivers than the coarser ECMWF fields. This granularity is particularly evident in the simulation of the boundary layer height, which, along with the diffusion coefficient discrepancies, significantly impacts air pollutant concentrations near the surface and their transport to the higher layers of the atmosphere.

The study underscores the importance of accurately representing the boundary layer height, as it plays a crucial role in the distribution and chemical transformation of pollutants. The higher boundary layer height simulated by HARMONIE facilitates the transport of pollutants to higher altitudes, where they can undergo chemical reactions leading to the formation of secondary pollutants. This phenomenon has implications for regional air quality, climate, and the understanding of long-range pollutant transport. Addressing the discrepancies in boundary layer height simulation requires further research, focusing on refining the model's parametrizations and processes related to boundary layer dynamics to enhance the simulation of pollutant dispersion across different atmospheric layers.

The analysis also points to a slight improvement in surface NO_2 concentrations when compared with observations from ground stations in the HARMONIE configuration, though it emphasizes that these findings do not significantly enhance our understanding of surface NO_2 levels. In terms of the statistics, an slight improvement for the performance in the surface NO_2 concentrations compared with ground stations was observed with the high-spatial resolution meteorology. The study calls for further examination of vertical transport processes and additional validation efforts, particularly with NO_2 profile measurements from MAX-DOAS. Highlighting the computational advantages and the need for high-spatial resolution in the HARMONIE configuration, the research suggests further development of LOTOS-EUROS to leverage these benefits fully.

Looking ahead, the study proposes using both the ECMWF and HARMONIE configurations in a data assimilation experiment with TROPOMI NO2 data. This approach aims to understand better the impact of uncertainties in the meteorology on the horizontal and vertical transport of contaminants, marking an essential step towards refining air quality models and improving our ability to predict and mitigate the effects of air pollution on the environment and public health.

Author contributions. Conceptualization, AYB and MvW; methodology, AYB; software; AYB and AS validation; analysis AYB and MvW and AS and HE formal resources MvW and HE and PS ; data curation AYB ; writing original draft preparation AYB ; writing review and editing MvW, AS ; visualization AYB; project administration MvW . All authors have read and agreed to the published version of the manuscript.

Competing interests. Authors declare that no competing interests are present

Code availability

The dataset used in this study was obtained from a public repository hosted on Zenodo, a widely-recognized open-access repository that facilitates research data sharing and collaboration. This particular dataset, accessible at https://doi.org/10.5281/zenodo.8431342, provides comprehensive data essential for our analysis. It was published in 2023 and support the findings of this research. To download the Cabauw data: https://dataplatform.knmi.nl/dataset/cesar-tower-meteo-lb1-t10-v1-2

Map data copyrighted by OpenStreetMap contributors and available from https://www.openstreetmap.org

The NO_2 data was downloaded for the ground stations at different places in the Netherlands from www.luchtmeetnet.nl

Acknowledgements. This research is supported by the NWO program gebruikersondersteuning under grant KNW19002 (Dutch collaborative network for air pollution monitoring using satellites)

Appendix: Appendix
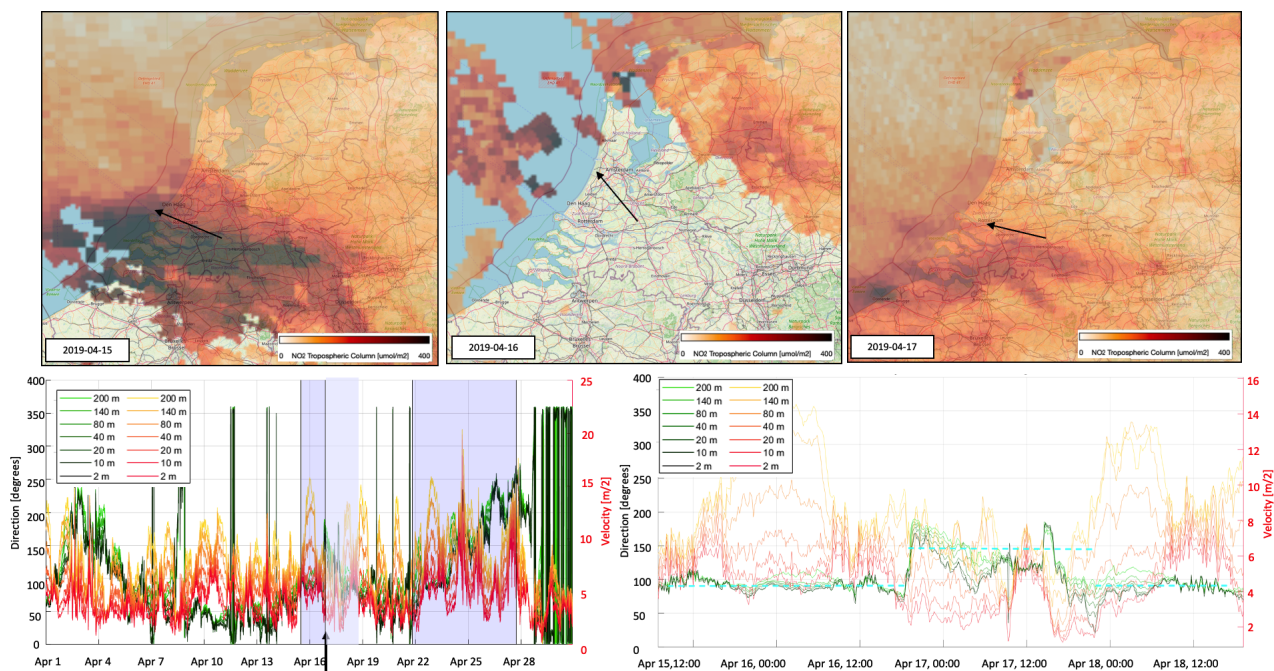
Figure 1. Transport plumes of NO$_2$ TROPOMI Tropospheric column observations compared with the CABAUW observations for wind direction and magnitude for 7 levels from 2 m to 200m 2019-04-15 to 2019-04-17. © OpenStreetMap contributors 2021. Distributed under the Open Data Commons Open Database License (ODbL) v1.0.
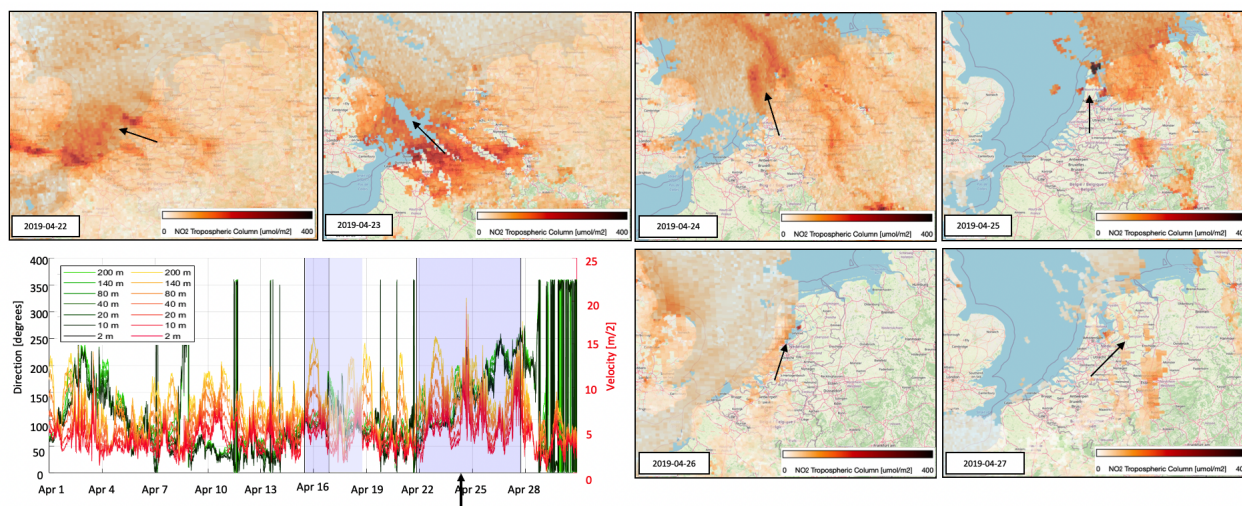
Figure 2. Transport plumes of NO$_2$ TROPOMI Tropospheric column observations compared with the CABAUW observations for wind direction and magnitude for 7 levels from 2 m to 200m from 2019-04-22 to 2019-04-27 in which a scenario of changing air mass direction drive the transport of contaminants. © OpenStreetMap contributors 2021. Distributed under the Open Data Commons Open Database License (ODbL) v1.0.

References

Apituley, A., Russchenberg, H., van der Marel, H., Bosveld, F., Boers, R., ten Brink, H., de Leeuw, G., Uijlenhoet, R., Arbresser-Rastburg, B., and Rockmann, T.: Overview of research and networking with ground based remote sensing for atmospheric profiling at the cabauw experimental site for atmospheric research (cesar)-the netherlands, in: IGARSS 2008-2008 IEEE International Geoscience and Remote Sensing Symposium, vol. 3, pp. III–903, IEEE, 2008.

Baas, P., Verzijlbergh, R., van Dorp, P., and Jonker, H.: Investigating energy production and wake losses of multi-gigawatt offshore wind farms with atmospheric large-eddy simulation, Wind Energy Science Discussions, pp. 1–28, 2022.

Bengtsson, L., Andrae, U., Aspelien, T., Batrak, Y., Calvo, J., de Rooy, W., Gleeson, E., Hansen-Sass, B., Homleid, M., Hortal, M., Ivarsson, K.-I., Lenderink, G., Niemelä, S., Nielsen, K. P., Onvlee, J., Rontu, L., Samuelsson, P., Muñoz, D. S., Subias, A., Tijm, S., Toll, V., Yang, X., and Ødegaard Køltzow, M.: The HARMONIE–AROME Model Configuration in the ALADIN–HIRLAM NWP System, Monthly Weather Review, 145, 1919 – 1935, https://doi.org/https://doi.org/10.1175/MWR-D-16-0417.1, 2017.

Boersma, K., Eskes, H., Dirksen, R., Van Der A, R., Veefkind, J., Stammes, P., Huijnen, V., Kleipool, Q., Sneep, M., Claas, J., et al.: An improved tropospheric NO 2 column retrieval algorithm for the Ozone Monitoring Instrument, Atmospheric Measurement Techniques, 4, 1905–1928, https://doi.org/https://doi.org/10.5194/amt-4-1905-2011, 2011.

Bosveld, F. C., Baas, P., Beljaars, A. C., Holtslag, A. A., de Arellano, J. V.-G., and Van De Wiel, B. J.: Fifty years of atmospheric boundary-layer research at Cabauw serving weather, air quality and climate, Boundary-Layer Meteorology, 177, 583–612, 2020.

Chang, T. Y.: Current concepts and applications of air quality simulation models, Environment International, 3, 337–351, 1980.

Clark, P., Roberts, N., Lean, H., Ballard, S. P., and Charlton-Perez, C.: Convection-permitting models: a step-change in rainfall forecasting, Meteorological Applications, 23, 165–181, 2016.

Ding, J.: Impact of HARMONIE high-resolution meteorological forecasts on the air quality simulations of LOTOS-EUROS, Royal Netherlands Meteorological Institute, 2013.

El-Harbawi, M.: Air quality modelling, simulation, and computational methods: a review, Environmental Reviews, 21, 149–179, 2013.

Engdahl, B. J. K., Thompson, G., and Bengtsson, L.: Improving the representation of supercooled liquid water in the HARMONIE-AROME weather forecast model, Tellus A: Dynamic Meteorology and Oceanography, 72, 1–18, 2020.

Escudero, M., Segers, A., Kranenburg, R., Querol, X., Alastuey, A., Borge, R., de la Paz, D., Gangoiti, G., and Schaap, M.: Analysis of summer O 3 in the Madrid air basin with the LOTOS-EUROS chemical transport model, Atmospheric Chemistry and Physics, 19, 14 211–14 232, 2019.

Fountoukis, C. and Nenes, A.: ISORROPIA II: a computationally efficient thermodynamic equilibrium model for K+– Ca2+– Mg2+– NH4+ – Na+– SO4 2− – NO3< su p>, Atmos. Chem. Phys, 7, 4639–4659, 2007.

Gibbon, J. and Holm, D. D.: Extreme events in solutions of hydrostatic and non-hydrostatic climate models, Philosophical Transactions of the Royal Society A: Mathematical, Physical and Engineering Sciences, 369, 1156–1179, 2011.

Haakenstad, H., Breivik, Ø., Furevik, B. R., Reistad, M., Bohlinger, P., and Aarnes, O. J.: NORA3: A nonhydrostatic high-resolution hindcast of the North Sea, the Norwegian Sea, and the Barents Sea, Journal of Applied Meteorology and Climatology, 60, 1443–1464, 2021.

Kalverla, P., Steeneveld, G.-J., Ronda, R., and Holtslag, A. A.: Evaluation of three mainstream numerical weather prediction models with observations from meteorological mast IJmuiden at the North Sea, Wind Energy, 22, 34–48, 2019.

Khan, S. and Hassan, Q.: Review of developments in air quality modelling and air quality dispersion models, Journal of Environmental Engineering and Science, 16, 1–10, 2020.

395 Knoop, S., Ramakrishnan, P., and Wijnant, I.: Dutch Offshore Wind Atlas Validation against Cabauw Meteomast Wind Measurements, Energies, 13, 6558, 2020.

Lawrence, M. G.: The relationship between relative humidity and the dewpoint temperature in moist air: A simple conversion and applications, Bulletin of the American Meteorological Society, 86, 225–234, 2005.

Lorenc, A. C. and Jardak, M.: A comparison of hybrid variational data assimilation methods for global NWP, Quarterly Journal of the Royal
400 Meteorological Society, 144, 2748–2760, 2018.

Manders, A. M., Builtjes, P. J., Curier, L., Denier van der Gon, H. A., Hendriks, C., Jonkers, S., Kranenburg, R., Kuenen, J. J., Segers, A. J., Timmermans, R., et al.: Curriculum vitae of the LOTOS–EUROS (v2. 0) chemistry transport model, Geoscientific Model Development, 10, 4145–4173, 2017.

Manders-Groot, A., Schaap, M., van Ulft, B., and van Meijgaard, E.: Coupling of the air quality model Lotus-Euros to the climate model
405 Racmo, National Research Programme Knowledge for Climate Nationaal Onderzoekprogramma Kennis voor Klimaat (KvK) All rights reserved, 2011.

Marseille, G.-J. and Stoffelen, A.: Toward Scatterometer Winds Assimilation in the Mesoscale HARMONIE Model, IEEE Journal of Selected Topics in Applied Earth Observations and Remote Sensing, 10, 2383 – 2393, https://doi.org/10.1109/JSTARS.2016.2640339, cited by: 10, 2017.

410 Menut, L., Bessagnet, B., Briant, R., Cholakian, A., Couvidat, F., Mailler, S., Pennel, R., Siour, G., Tuccella, P., Turquety, S., et al.: The CHIMERE v2020r1 online chemistry-transport model, Geoscientific Model Development, 14, 6781–6811, 2021.

Pielke, R. A. and Uliasz, M.: Use of meteorological models as input to regional and mesoscale air quality models—limitations and strengths, Atmospheric environment, 32, 1455–1466, 1998.

SAITO, K., ichi ISHIDA, J., ARANAMI, K., HARA, T., SEGAWA, T., NARITA, M., and HONDA, Y.: Nonhydrostatic Atmo-
415 spheric Models and Operational Development at JMA, Journal of the Meteorological Society of Japan. Ser. II, 85B, 271–304, https://doi.org/10.2151/jmsj.85B.271, 2007.

Schaap, M., Van Loon, M., Ten Brink, H., Dentener, F., and Builtjes, P.: Secondary inorganic aerosol simulations for Europe with special attention to nitrate, Atmospheric Chemistry and Physics, 4, 857–874, 2004.

Schaap, M., Timmermans, R. M., Roemer, M., Boersen, G., Builtjes, P., Sauter, F., Velders, G., and Beck, J.: The LOTOS? EUROS model:
420 description, validation and latest developments, International Journal of Environment and Pollution, 32, 270–290, 2008.

Thürkow, M., Kirchner, I., Kranenburg, R., Timmermans, R., and Schaap, M.: A multi-meteorological comparison for episodes of PM10 concentrations in the Berlin agglomeration area in Germany with the LOTOS-EUROS CTM, Atmospheric Environment, 244, 117 946, 2021.

van Stratum, B., Theeuwes, N., Barkmeijer, J., van Ulft, B., and Wijnant, I.: A One-Year-Long Evaluation of a Wind-Farm Parameterization
425 in HARMONIE-AROME, Journal of Advances in Modeling Earth Systems, 14, e2021MS002 947, 2022.

Verzijlbergh, R.: Atmospheric flows in large wind farms, Europhysics News, 52, 20–23, 2021.

Viana Jiménez, S. and Díez Muyo, M. V.: Procesos de superficie en Harmonie-Arome y su importancia en procesos atmosféricos, Sexto simposio nacional de prediccion- Memorial Antonio Mestres, 2019.

Wichink Kruit, R., Schaap, M., Sauter, F., Van Zanten, M., and Van Pul, W.: Modeling the distribution of ammonia across Europe including
430 bi-directional surface–atmosphere exchange, Biogeosciences, 9, 5261–5277, 2012.